

Estimation of the release time of solar energetic particles near the Sun

Yang Wang¹ and Gang Qin¹

ywang@spaceweather.ac.cn; gqin@spaceweather.ac.cn

Received _____; accepted _____

Not to appear in Nonlearned J., 45.

¹State Key Laboratory of Space Weather, National Space Science Center, Chinese Academy of Sciences, Beijing 100190, China

ABSTRACT

This paper investigates the onset time of Solar Energetic Particle (SEP) events with numerical simulations, and analyses the accuracy of the Velocity Dispersion Analysis (VDA) method. Using a 3-dimensional focused transport model, we calculate the fluxes of protons observed at 1 AU equatorial plane in energy range between 10 MeV and 80 MeV. In particular, three models are used to describe different SEP sources produced by flare or coronal shock, and the effects of particle perpendicular diffusion in the interplanetary space are also studied. We have the following findings: (1) When the observer is connected to the source by interplanetary magnetic field, the effects of particles propagating in the solar atmosphere and perpendicular diffusion in the interplanetary space have little influence on the onset time of SEP fluxes and the VDA results; (2) If SEPs are accelerated by a flare, the VDA method can not be used when the observer is far from SEP source, because particles must spend some time on leaving the source to the observer's field line with the effect of propagating in the solar atmosphere or perpendicular diffusion in the interplanetary space; and (3) If SEPs are accelerated by a large coronal shock, observer's location would change the VDA results unless the time profile of SEP source is the same at different point of the shock front.

Subject headings: Sun: energetic particles — Sun: flare — Sun: shock — Sun: onset time

1. Introduction

Solar Energetic Particles (SEPs) were first reported by Forbush (1946). Since coronal mass ejection (CME) was not discovered at that time, SEPs were assumed to be accelerated by solar flare. If this holds true, it is reasonable to assume that the size of SEPs source is close to that of flare. However, some SEP events could be simultaneously observed by multi-spacecraft with very wide spatial distribution which could be much wider than the size of flare. In order to interpret this phenomenon, two scenarios were proposed: (1) particles can propagate in the solar atmosphere (Wibberenz et al. 1989); and (2) particles can cross the interplanetary magnetic field (IMF) lines in the interplanetary space with perpendicular diffusion (McKibben 1972). But later the SEP community realized that CMEs are important for particle acceleration, especially in some large SEP events (Mason et al. 1984; Gosling 1993; Zank et al. 2000; Li et al. 2003). As a result, besides the former two scenarios, the third one was proposed: the wide spread of SEPs can be explained by that SEPs are accelerated by large scale shocks. However, large SEP events are usually associated with flares and CMEs, so the role of flare and shock in acceleration process of SEPs is still in debate. For historical development of the studies on SEP source, please refer to the review articles by Reames (1999) and Reames (2013).

Because of the effects of particle transport, it is difficult to distinguish signatures of different accelerators in SEP fluxes at 1 AU. However, SEP fluxes observed in the interplanetary space show velocity dispersion at the onset time. The Velocity Dispersion Analysis (VDA) method has been used widely to investigate the SEP acceleration and transport process (Krucker et al. 1999; Krucker & Lin 2000; Reames 2009; Li et al. 2013). This method assumes that the first arriving particles move along the magnetic field lines, and the scattering can be ignored. With these assumptions, the SEP release time near the Sun and the interplanetary path length can be determined by using the onset time of different energy particles. To compare the release time with the electromagnetic signature of SEP source, the SEP source can be identified .

It has been known for a long time that when the observer is far from the magnetic connection point of the source on the Sun, the onset time of SEPs' flux shows a delay (Ma Sung & Earl 1978; Van Hollebeke et al. 1975). This would leads to changes in the results of VDA method. Krucker et al. (1999) calculated the release time near the Sun and path length in the interplanetary space of SEPs with 12 short electron events observed by Wind spacecraft. The result of VDA method indicates two kinds of electron events. In the first kind of events, the electron release time is extremely close to the onset of a radio type III burst when the observer is connected to the flare. In the second kind of events, the electrons are released much later (e.g., half an hour) than the onset of the type III burst when the observer is disconnected from the flare. Huttunen-Heikinmaa et al. (2005) studied the release time of MeV/n protons and heliums observed by SOHO spacecraft. They found that the delay in SEPs release time derived from VDA method is related to the poor magnetic connection between the flare site and the spacecraft. For extremely high energy particle events, Reames (2009) studied the onset time of ion fluxes in ground-level solar energetic particle events. They found that the time difference between the solar particle release time and the onset time of metric type II radio burst increases with the angular distance of the observer's magnetic foot-point and the source increase.

According to different heliographic latitude observation, Zhang et al. (2003) analyzed an SEP event simultaneously observed by Ulysses and GOES spacecraft. The GOES spacecraft is located at the ecliptic plane, while the Ulysses is located at 62° South. The release time derived from GOES data is consistent with the onset of soft X-ray flux, and the path length is also close to the Parker spiral. To the contrary, the release time derived from Ulysses data is 3 hours later than the onset of soft X-ray, and the path length is much longer than the Parker spiral. The further studies were done by Dalla et al. (2003a,b), which analysed 9 SEP events observed by Ulysses at high latitudes among which 8 events are observed at more than 60° latitude, and 1 events is observed at 47.9° latitude. Dalla et al. (2003a,b) found that the path lengths at Ulysses are 1.06 to 2.45 times the length of Parker spiral, and the particle release time is between 100 and

350 min later than the release time derived from SOHO and Wind measurements. The delay in particle release time increases with the latitudinal difference $\Delta\theta$ between the spacecraft and the flare. Based on the observation results derived from in-ecliptic and high latitudes measurements, we can conclude that the delay in the release time is related to the poor connection between the source and spacecraft.

In order to use the VDA method more reasonably, many works have been done to investigate the validity of this method. The following are the main conclusions: Firstly, when the parallel mean free path (MFP) is large enough ($\lambda_{\parallel} > 0.3$ AU), interplanetary scattering can be ignored (Kallenrode & Wibberenz 1990; Lintunen & Vainio 2004; Diaz et al. 2011). Secondly, when the background level is below 0.01% of the peak intensity of flux, the onset time of SEP event can be determined quite accurately (Sáiz et al. 2005). In the above works, the interplanetary scattering and background level effects in the release time have been studied in detail. In this work, we study how different source models and perpendicular diffusion affects the onset time of SEP and the VDA results. In section 2 we describe the SEP transport model. In Section 3 we show the simulation results. In Section 4 we discuss the simulation and observation results, and summarize our results.

2. Model

We model the transport of SEPs following previous research (e.g., Qin et al. 2006; Zhang et al. 2009; He et al. 2011; Wang et al. 2012; Qin et al. 2013; Zuo et al. 2013). A three-dimensional focused transport equation is written as (Skilling 1971; Schlickeiser 2002; Qin et al. 2006; Zhang et al. 2009)

$$\begin{aligned} \frac{\partial f}{\partial t} &= \nabla \cdot (\kappa_{\perp} \cdot \nabla f) - \left(v\mu \hat{\mathbf{b}} + \mathbf{V}^{sw} \right) \cdot \nabla f + \frac{\partial}{\partial \mu} \left(D_{\mu\mu} \frac{\partial f}{\partial \mu} \right) \\ &+ p \left[\frac{1 - \mu^2}{2} \left(\nabla \cdot \mathbf{V}^{sw} - \hat{\mathbf{b}} \hat{\mathbf{b}} : \nabla \mathbf{V}^{sw} \right) + \mu^2 \hat{\mathbf{b}} \hat{\mathbf{b}} : \nabla \mathbf{V}^{sw} \right] \frac{\partial f}{\partial p} \end{aligned}$$

$$-\frac{1-\mu^2}{2} \left[-\frac{v}{L} + \mu \left(\nabla \cdot \mathbf{V}^{sw} - 3 \hat{\mathbf{b}} \hat{\mathbf{b}} : \nabla \mathbf{V}^{sw} \right) \right] \frac{\partial f}{\partial \mu}, \quad (1)$$

where $f(\mathbf{x}, \mu, p, t)$ is the gyrophase-averaged distribution function, \mathbf{x} is the position in a non-rotating heliographic coordinate system; p , μ , and v are the momentum, particle pitch-angle cosine, and speed, respectively, in the solar wind frame; t is the time; $\mathbf{V}^{sw} = V^{sw} \hat{\mathbf{r}}$ is the solar wind velocity; $\hat{\mathbf{b}}$ is a unit vector along the local magnetic field, and L is the magnetic focusing length given by $L = (\hat{\mathbf{b}} \cdot \nabla \ln B_0)^{-1}$ with B_0 being the magnitude of the background magnetic field. This equation includes many important particle transport effects such as particle streaming along field line, magnetic focusing in the diverging IMF, adiabatic cooling in the expanding solar wind, and the diffusion coefficients parallel and perpendicular to the IMF. Here, we use the Parker field model for the IMF, and the solar wind speed is 400 km/s.

The relationship of the $D_{\mu\mu}$ and parallel mean free path λ_{\parallel} is written as (Jokipii 1966; Hasselmann 1968; Earl 1974)

$$\lambda_{\parallel} = \frac{3v}{8} \int_{-1}^{+1} \frac{(1-\mu^2)^2}{D_{\mu\mu}} d\mu, \quad (2)$$

and parallel diffusion coefficient κ_{\parallel} can be written as $\kappa_{\parallel} = v\lambda_{\parallel}/3$.

We follow the model of pitch angle diffusion coefficient from Beeck & Wibberenz (1986), see also (Qin et al. 2005)

$$D_{\mu\mu} = D_0 v p^{q-2} \left\{ |\mu|^{q-1} + h \right\} (1 - \mu^2), \quad (3)$$

where the constant D_0 controls the magnetic field fluctuations level. The constant q is chosen 5/3 for a Kolmogorov spectrum type of the power spectral density of magnetic field turbulence in the inertial range. Furthermore, a larger value of $h = 0.01$ is chosen for non-linear effect of pitch angle diffusion at $\mu = 0$ in the solar wind (Qin & Shalchi 2009; Qin & Shalchi 2014).

The relation of the particle momentum and the perpendicular diffusion coefficient is set as

$$\kappa_{\perp} = \kappa_0 \left(\frac{p}{1 \text{ GeV } c^{-1}} \right)^{1/3} \left(\mathbf{I} - \hat{\mathbf{b}} \hat{\mathbf{b}} \right) \quad (4)$$

where κ_0 is a constant, and p is particle momentum. The perpendicular diffusion coefficient is proportional to parallel one,

$$\kappa_{\perp} = a\kappa_{\parallel} \quad (5)$$

where we set $a = 0.01$ in our simulations.

We use boundary values to model the particle injection from the source, and the boundary condition is chosen as the following form

$$f_b(z \leq 0.05\text{AU}, E_k, \theta, \varphi, t) = a \frac{E_k^{-\gamma}}{p^2} \xi(t, \theta, \varphi), \quad (6)$$

$$\xi(t, \theta, \varphi) = \begin{cases} \frac{1}{t} \exp \left[-\frac{t_c}{t} \left(\frac{\phi_s}{\phi_0} \right)^2 - \frac{t}{t_l} \right] H(\phi_s - |\phi(\theta, \varphi)|) & \text{Case 1,} \\ \left\{ \frac{1}{t} \exp \left[-\frac{t_c}{t} \left(\frac{\phi_s}{\phi_0} \right)^2 - \frac{t}{t_l} \right] H(\phi_s - |\phi(\theta, \varphi)|) + \right. \\ \left. \frac{1}{t} \exp \left[-\frac{t_c}{t} \left(\frac{\phi(\theta, \varphi)}{\phi_0} \right)^2 - \frac{t}{t_l} \right] [1 - H(\phi_s - |\phi(\theta, \varphi)|)] \right\} & \text{Case 2,} \\ \frac{1}{t} \exp \left(-\frac{t_c}{t} - \frac{t}{t_l} \right) \exp \left(-\frac{|\phi(\theta, \varphi)|}{\phi_0} \right) H(\phi_s - |\phi(\theta, \varphi)|) & \text{Case 3.} \end{cases}$$

Here the particles are injected from the SEP source near the Sun. $\phi(\theta, \varphi)$ is the angle between the source center and any point (θ, φ) near the Sun where the particles are injected. We use three models to describe different scenarios: SEPs are accelerated by a flare, and particles do not propagate in the solar atmosphere in case 1; SEPs are accelerated by a flare, and particles can propagate in the solar atmosphere in case 2; and SEPs are accelerated by a coronal shock in case 3. The flare source model in case 1 and 2 is obtained following Reid (1964), and the shock model in case 3 is obtained following Kallenrode & Wibberenz (1997). $H(x)$ is the Heaviside step function. ϕ_s is used to control the angular width of the source. ϕ_0 describes how the source intensity decreases towards the flank of the source. E_k is energy of the particles, and γ is the spectral index of source particles. t_c and t_l are time constants to indicate the rise and decay timescales, respectively. Here, we set a typical value of $\gamma = -3$ for the spectral index of source particles.

We use a time-backward Markov stochastic process method to solve the transport equation (1) (Zhang 1999). The initial-boundary value problem of the SEP transport equation can be

reformulated to stochastic differential equations, so it can be solved by a Monte-Carlo simulation of Markov stochastic process, and the SEP distribution function can be derived. In this method, we trace particles from the observation point back to the injection time from the SEP source. Only those particles in the source region at the initial time contribute to the statistics. For detailed description of the method, please refer to Qin et al. (2006).

3. Results

Note that the interplanetary field is the Parker field. The inner boundary is 0.05 AU, and outer boundary is 50 AU. We set a typical value of $\lambda_{||} = 0.126$ AU for 10 MeV particles. Base on the simulation results of Diaz et al. (2011), the interplanetary scatterings can not be ignored in this case. The ratio of perpendicular mean free path to parallel one is 0.01. We choose different t_c and t_l to study different duration of the source. We set $t_c = 0.02$ day (0.48 hour) and $t_l = 0.05$ day (1.2 hours) as a short duration, and set $t_c = 0.1$ day (2.4 hours) and $t_l = 0.25$ day (6 hours) as a long duration case. In our simulations, the source rotates with the Sun.

Before we can determine the detected onset time from the simulated time profiles, we have to define a background level of the flux. In a real SEP event, this background may be either due to the level of galactic cosmic rays or previous SEP event. In this paper, we choose the background level as a constant fraction A of the maximum intensity. In each energy channel, we set the background fraction A as 10^{-5} , 10^{-3} , and 10^{-1} , corresponding to a low background level, middle background level, and high background level, respectively.

3.1. Particles Do Not Propagate in the Solar Atmosphere

In the following subsections, we use the source model as shown in the case 1 of Equation (6), and particles do not propagate in the solar atmosphere. In addition, ϕ_s and ϕ_0 are set to be 15° .

3.1.1. *Effect of Perpendicular Diffusion on the Onset Time of SEP Event*

Figure 1 (a) shows time profiles of 10 MeV protons' omnidirectional flux, in the cases with and without perpendicular diffusion. The source duration is set as $t_c = 0.1$ day and $t_l = 0.25$ day as a long duration. The solid line indicates the case with perpendicular diffusion, and the dash-dotted line indicates the case without perpendicular diffusion. The observer is located at equator and 0° longitude, and the observer's field line is connected to the center of source near the Sun directly. Comparing the time profiles of flux, we can find the observed flux is smaller with the perpendicular diffusion. In this case, the particles can leave the field lines, and transport in the whole space. Figure 1 (b) shows the time profiles of flux normalized by the peaks. As one can see, the onset times are much the same with and without perpendicular diffusion. The two cases could not possibly be distinguished observationally. In order to check the onset time, we also show the normalized flux in the following cases.

3.1.2. *Different Source Durations*

Figure 2 (a) shows time profiles of 10 MeV protons' omnidirectional flux, in the cases of different source durations. The observer is located at equator and 0° longitude, and the observer's field line is connected to the center of source near the Sun directly. The solid line indicates the case with the short duration source, and the dash-dotted line indicates the case with the long duration source. Comparing the time profiles of flux, the flux rises more quickly during the beginning in the case of short duration source. Figure 2 (b) shows the time profiles of normalized flux. As one can see, the onset time of flux is earlier with the short duration.

3.1.3. *Observers at Different Locations*

Figure 3 (a) shows time profiles of 10 MeV protons' omnidirectional flux detected by three observers. The source duration is set as $t_c = 0.1$ day and $t_l = 0.25$ day. The observers are located at the equator 0° longitude (solid line), 50° west longitude (dash-dotted line), and 50° east longitude (dash line), respectively. When an observer is located at equator 0° longitude, it is connected to the center of source directly by IMF. In this case, energetic particles can arrive at the observer's location by following the field lines. The 50° west and 50° east indicate that the center of source is 50° west and 50° east to the IMF footpoint of the observers, respectively. In these cases, the two observers' field lines are disconnected from the SEP source, because the half width of source is only 15° . Therefore energetic particles can only be detected by the observers with the effect of perpendicular diffusion during the onset time. According to the three observers, the peak of flux is the largest when the observer is connected directly to the source by IMF, and it is the smallest when the observer is located at 50° west. Due to the effect of convection, the particles rotate with the Sun after they are emitted. More particles are injected to the field line of observer at 50° east than that in the case of 50° west. As a result, the flux of 50° west is smaller than that of 50° east. This effect would lead to east-west asymmetry of SEPs distribution in the interplanetary space. Figure 3 (b) shows time profiles of normalized omnidirectional flux for the cases in Figure 3 (a). According to the three observers, the onset time is earliest when the observer is connected to the source, and it is latest in the case of 50° east.

3.1.4. *Effect of Perpendicular Diffusion on the VDA Method Results*

In last subsection, we have briefly studied the effect of perpendicular diffusion on the onset time of SEP flux. In this subsection, we will study how the perpendicular diffusion affects the VDA method results. The VDA method assumes that the first observed particles are the zero pitch angle particles travelling without scattering. If this holds, the transport time for SEPs is given by

$$t_o - t_i = \frac{l}{v}, \quad (7)$$

here, l represents the field line length, t_o is the onset time of SEP flux, t_i is the release time of particles on the source, and v is speed of energetic particles.

Figure 4 (a) and (b) show the dispersion of the onset time changes with c/v according to different source durations, where the observers are located at equator 0° longitude, and the observer's field line is connected directly to the center of source near the Sun. Here, we get time profiles of SEP fluxes with simulations for four energy channels, 10 MeV, 20 MeV, 40 MeV, and 80 MeV. We set the SEP background as 10^{-5} of the flux peak. From SEP fluxes we obtain the onset times as the times when fluxes rise above the background. As one can see, the onset time increases linearly with c/v . Based on the results of data fitting, the release time near the Sun and interplanetary field length can be derived. The only difference between Figure 4 (a) and (b) is the source duration times.

With different observing locations, background levels, and source duration times, the calculated onset times and path lengths from the VDA method with simulation data are listed in Table 1. In this study, the observers are all located at 1 AU equatorial plane, but at different longitudes (0° , 50° west, and 50° east). When the observer is connected to the source, we have the following findings. In the cases of short source duration (cases 1, 2, and 3), the VDA release times are very close to the injection times on the source (less than 3 minutes). In the cases of long source duration (cases 4, 5, and 6), however, the VDA release times are much later than the real release times. On the other hand, when the observer is disconnected from the source, the onset time of SEP flux is later than the case when the observer is connected to the source. Therefore, the VDA results are generally much worse when the observer is disconnected from the source with some exceptions. For example, in W50 of case 4, the release time of VDA result is very close to the injection time on the source (less than 2 minutes). Obviously, this result is obtained fortuitously,

and it can not be taken as an indication that the VDA method is valid. In all six cases (case 1, 2, 3, 4, 5 and 6), the path lengths obtained from VDA method are longer than the real ones from Parker spiral. Even when the observer is connected to the center of flare with short duration source and low background SEP level, the path length is still larger than that of Parker spiral. This is because the scatterings in the interplanetary space could not be ignored due to the value of mean free path used in our simulation. Beside the scatterings in the interplanetary space, the source duration, source location, and SEP background level also affect the path length result of VDA. Therefore, in the case 6 of Table 1, the path lengths are much larger than that of Parker spiral.

3.2. Different Source and Transport Models

Figure 5 shows time profiles of 10 MeV protons' normalized omnidirectional flux in the cases with different source models. The source parameter ϕ_0 is set to be 15° in all the three cases. The solid line indicates that particles do not propagate in the solar atmosphere with case 1 of Equation (6) ($\phi_s = 15^\circ$). The dashed line indicates that particles can propagate in the solar atmosphere with case 2 of Equation (6) ($\phi_s = 15^\circ$). The dash-dotted line indicates that particles are accelerated by a coronal shock with case 3 of Equation (6) ($\phi_s = 60^\circ$). In all of the three cases, the observer is located at 1 AU equatorial plane, and is connected to the center of source. The time profiles are similar during the rising phase in all cases. As a result, when the observer is connected to the center of source, the spatial distribution of source does not affect the VDA results.

Figure 6 shows time profiles of 10 MeV protons' omnidirectional flux in the cases with different propagation models. In all cases, the observer is located at 1 AU equatorial plane, and is $E50^\circ$ to the center of SEP source with $\phi_s = 15^\circ$. The source parameter ϕ_0 is set to be 15° and 5° in Figure 6 (a) and (b), respectively. The source model of solid lines and dashed lines is in case 2 of Equation (6). The source model of dash-dotted line is in case 1 of Equation (6), which indicates that particles do not propagate in the solar atmosphere. In addition, the solid and dash-dotted lines

indicate that particles propagate in the interplanetary space with perpendicular diffusion, while the dashed lines indicate that particles without perpendicular diffusion. In Figure 6 (a), the flux indicated by the solid line is the largest, and that indicated by the dash-dotted line is the smallest. With the parameters in this case, the effect of particles propagation in the solar atmosphere is stronger than that of perpendicular diffusion in the interplanetary space. In Figure 6 (b), the flux indicated by the solid line is the largest, and that indicated by the dashed line is the smallest. With the parameters in this case, the effect of particles propagation in the solar atmosphere is weaker than that of perpendicular diffusion in the interplanetary space. Comparing these two panels, the time scale of rising phase of flux indicated by solid line in the panel (a) is smaller than that in the panel (b).

3.3. Particles Propagate in the Solar Atmosphere

Figure 7 (a) shows time profiles of 10 MeV protons' omnidirectional flux observed at different locations, while Figure 7 (b) shows the normalized fluxes. We use the source model as shown in the case 2 of Equation (6). Here, particles produced by flare can propagate in the solar atmosphere, and they can also cross the field lines with perpendicular diffusion in the interplanetary space. The source parameter ϕ_0 and ϕ_s are set to be 15° . In this case, the effect of particles propagating in the solar atmosphere is stronger than that of perpendicular diffusion in the interplanetary space. Three observers are located at 1 AU equatorial plane, but at different longitudes ($E50^\circ$, 0° , and $W50^\circ$). According to the observers, the flux is the largest when the observer is connected to the center of source, and is the smallest when the observer is located at $W50^\circ$. Figure 7 (b) reveals that the onset times of three fluxes are different. In the source model, when ϕ is larger than 15° , the time profile of SEP source changes with ϕ . As a result, the time profiles of SEP flux observed at longitude $E50^\circ$ and $W50^\circ$ increase more slowly than that in the case of longitude 0° . In this case, when the observer is far from the center of source ($\phi > 15^\circ$), the

angular distance should affect the VDA results.

3.4. Particles Accelerated by A Large Corona Shock

Figure 8 is similar to Figure 7 but with different SEP source near the Sun. We use the SEP source model as shown in the case 3 of Equation (6). Particles are accelerated by a corona shock, and they can also cross the field lines with perpendicular diffusion in the interplanetary space. The source parameter ϕ_s is set to be 60° , and ϕ_0 is set to be 15° . Three observers are located at E 50° , 0° , and W 50° . In this case, the observers are connected to the source by magnetic field lines. Since the time profile of source does not change with ϕ in our model, the time profiles of fluxes detected by three observers are similar during the rising phase in Figure 8 (b). As a result, the angular distance between the center of source and observer should not affect the VDA results when observer is connected to the source. However, if the time profile of SEP source changes with angular distance, the time profiles of flux detected by the observers should be different. This conclusion could be deduced from the results in Figure 2 or Figure 7. In this case, the VDA results should change with the angular distance between the center of source and observer.

4. Discussion and Conclusions

In this paper, we discuss the uncertainty of the simple assumptions of VDA method. Firstly, the ignorance of interplanetary scattering is not consistent with theory and simulation results of particle transport (Kallenrode & Wibberenz 1990; Lintunen & Vainio 2004; Diaz et al. 2011). Secondly, the onset time of SEP event is hard to be determined in practical applications, since it can be significantly delayed by the background level (Sáiz et al. 2005). Thirdly, particles can cross the field lines when they transport in the space. The perpendicular diffusion plays a very important role in the release time determination, especially when the observer’s field line is disconnected

from the source (Zhang et al. 2009; Qin et al. 2011; He et al. 2011). Fourthly, different source models affect the accuracy of results of VDA method. For example, particles accelerated by a flare may directly propagate in the solar atmosphere (Wibberenz et al. 1989); and a large shock could provide a very wide source (Mason et al. 1984; Gosling 1993; Zank et al. 2000; Li et al. 2003).

By numerically solving the focused Fokker-Planck equation, we have calculated SEPs' intensity time profiles including the perpendicular diffusion. We set different source duration and background level to study the onset times observed by observers. Comparing the time profiles of SEP fluxes observed at different locations, we have studied the effect of different source models and perpendicular diffusion on the onset times of SEP events, and its influence on the onset time of SEP flux and the VDA method results. Our new findings are the following.

(1) If SEPs are produced by a solar flare, they can spread much wider than the source region by two possible mechanisms. One is particles propagation in the solar atmosphere, the other is particles crossing of the field lines in the interplanetary space with perpendicular diffusion. In this case, the VDA results can be affected by the above two mechanisms when the observer is not connected to the source at initial time. In addition, due to the effect of convection, more particles are injected in the field line of observer at east longitude than that of the observer at west longitude. Therefore, the flux of the observer at east longitude is larger than that of the observer at west longitude. This effect would lead to east-west asymmetry of SEPs distribution in the interplanetary space.

(2) When the observer is connected to the source by IMF, comparing the time profiles of fluxes in the cases with and without perpendicular diffusion, or with and without particles propagation in the solar atmosphere, the onset times are much the same. In this case, the perpendicular diffusion in the interplanetary space and propagation in the solar atmosphere do not affect the results of VDA significantly. The results obtained by previous simulations, which didn't include these two mechanisms (Kallenrode & Wibberenz 1990; Lintunen & Vainio 2004;

Sáiz et al. 2005; Diaz et al. 2011), still holds when these two mechanisms are included.

(3) If SEPs accelerated by a solar flare can not propagate in the solar atmosphere, the SEP source region is approximate to the size of solar flare. In this case, when the observer is disconnected from the source by IMF, the energetic particles can be detected with the effect of the perpendicular diffusion. The onset time is later when the observer is disconnected from the source than that when the observer is connected to the source. The release time and the path length obtained from the VDA method are much different from the real values except some fortuitous cases.

(4) If SEPs accelerated by a solar flare can propagate in the solar atmosphere, the SEP source region should be larger than the size of solar flare as times go by. When the observer is far from the SEP source at the initial time, particles will spend some time on leaving the source to the observer's field line. As a result, the time scale of rising phase of flux is larger than that in the case when the observer is connected to the center of source. Therefore, the VDA results would change with the angular distance between the center of the source and the observer.

(5) If SEPs are accelerated by a large scale corona shock, the source can cover very wide region due to the size of corona shock. The observers located at different locations can be connected to the Sun simultaneously. If the time profile of SEP source does not change with the angular distance between the foot-point of observer's magnetic field line and the center of the source, the onset time of fluxes observed at different locations could be much the same. In this case, the VDA results do not change with the angular distance. Otherwise, if the time profile of SEP source changes with the angular distance, the onset time of SEP flux and the VDA results will also change with it.

(6) Due to the value of particle mean free path used in our simulations, the scatterings in the interplanetary space could not be ignored. Therefore, the path lengths obtained from VDA method are longer than that of Parker spiral in our simulations. Even when the observer is connected to

the center of source with short duration source and low background SEP level, the path length is still larger than that of Parker spiral. Beside the scatterings in the interplanetary space, the source duration, source location, and SEP background level also affect the path length of VDA results.

(7) In our simulations, the VDA results are significantly influenced by the location and size of SEP source. As it is shown in previous studies (Kallenrode & Wibberenz 1990; Lintunen & Vainio 2004; Sáiz et al. 2005; Diaz et al. 2011), the VDA results are also significantly affected by the time profile of source, parallel mean free path, and background level. As a result, the VDA method is applicable in some SEP events which meet the following conditions, such as, short source duration, large parallel mean free path, low background level, and good connection between the observer and the source.

The authors thank the anonymous referee for valuable comments. We are partly supported by grants NNSFC 41374177, NNSFC 41125016, and NNSFC 41304135, the CMA grant GYHY201106011, and the Specialized Research Fund for State Key Laboratories of China. The computations were performed by Numerical Forecast Modeling R&D and VR System of State Key Laboratory of Space Weather and Special HPC work stand of Chinese Meridian Project.

REFERENCES

Beeck, J., & Wibberenz, G. 1986, *ApJ*, 311, 437

Dalla, S., et al. 2003a, *Annales Geophysicae*, 21, 1367

—. 2003b, *Geophys. Res. Lett.*, 30, 8035

Diaz, I., Zhang, M., Qin, G., & Rassoul, H. K. 2011, in International Cosmic Ray Conference, Vol. 10, 40

Earl, J. 1974, *The Astrophysical Journal*, 193, 231

Forbush, S. E. 1946, *Physical Review*, 70, 771

Gosling, J. T. 1993, *J. Geophys. Res.*, 98, 18937

Hasselmann, K. 1968, *Z. Geophys.*, 34, 353

He, H.-Q., Qin, G., & Zhang, M. 2011, *The Astrophysical Journal*, 734, 74

Huttunen-Heikinmaa, K., Valtonen, E., & Laitinen, T. 2005, *A&A*, 442, 673

Jokipii, J. R. 1966, *ApJ*, 146, 480

Kallenrode, M., & Wibberenz, G. 1997, *J. Geophys. Res.*, 102, 22311

Kallenrode, M.-B., & Wibberenz, G. 1990, in International Cosmic Ray Conference, Vol. 5, International Cosmic Ray Conference, 229–+

Krucker, S., Larson, D. E., Lin, R. P., & Thompson, B. J. 1999, *ApJ*, 519, 864

Krucker, S., & Lin, R. P. 2000, *ApJ*, 542, L61

Li, C., Firoz, K. A., Sun, L., & Miroshnichenko, L. 2013, *The Astrophysical Journal*, 770, 34

Li, G., Zank, G., & Rice, W. 2003, *Journal of Geophysical Research: Space Physics (1978–2012)*, 108

Lintunen, J., & Vainio, R. 2004, *A&A*, 420, 343

Ma Sung, L. S., & Earl, J. A. 1978, *ApJ*, 222, 1080

Mason, G., Gloeckler, G., & Hovestadt, D. 1984, *The Astrophysical Journal*, 280, 902

McKibben, R. B. 1972, *Journal of geophysical research*, 77, 3957

Qin, G., He, H.-Q., & Zhang, M. 2011, *ApJ*, 738, 28

Qin, G., & Shalchi, A. 2009, *The Astrophysical Journal*, 707, 61

Qin, G. & Shalchi, A. 2014, *Physics of Plasmas*, 21, 042906

Qin, G., Wang, Y., Zhang, M., & Dalla, S. 2013, *The Astrophysical Journal*, 766, 74

Qin, G., Zhang, M., Dwyer, J., Rassoul, H., & Mason, G. 2005, *The Astrophysical Journal*, 627, 562

Qin, G., Zhang, M., & Dwyer, J. R. 2006, *Journal of Geophysical Research (Space Physics)*, 111, 8101

Reames, D. V. 1999, *Space Sci. Rev.*, 90, 413

Reames, D. V. 2009, *The Astrophysical Journal*, 706, 844

—. 2013, *Space Science Reviews*, 175, 53

Reid, G. C. 1964, *Journal of Geophysical Research*, 69, 2659

Sáiz, A., Evenson, P., Ruffolo, D., & Bieber, J. W. 2005, *ApJ*, 626, 1131

Schlickeiser, R. 2002, *Cosmic ray astrophysics* (Springer)

Skilling, J. 1971, *ApJ*, 170, 265

Van Hollebeke, M., Sung, L. M., & McDonald, F. 1975, *Solar Physics*, 41, 189

Wang, Y., Qin, G., & Zhang, M. 2012, *The Astrophysical Journal*, 752, 37

Wibberenz, G., Kecskemeti, K., Kunow, H., Somogyi, A., Iwers, B., Logachev, Y. I., & Stolpovskii, V. 1989, *Solar physics*, 124, 353

Zank, G. P., Rice, W. K. M., & Wu, C. C. 2000, *J. Geophys. Res.*, 105, 25079

Zhang, M. 1999, *ApJ*, 513, 409

Zhang, M., McKibben, R. B., Lopate, C., Jokipii, J. R., Giacalone, J., Kallenrode, M.-B., & Rassoul, H. K. 2003, *Journal of Geophysical Research (Space Physics)*, 108, 1154

Zhang, M., Qin, G., & Rassoul, H. 2009, *ApJ*, 692, 109

Zuo, P., Zhang, M., & Rassoul, H. K. 2013, *The Astrophysical Journal*, 767, 6

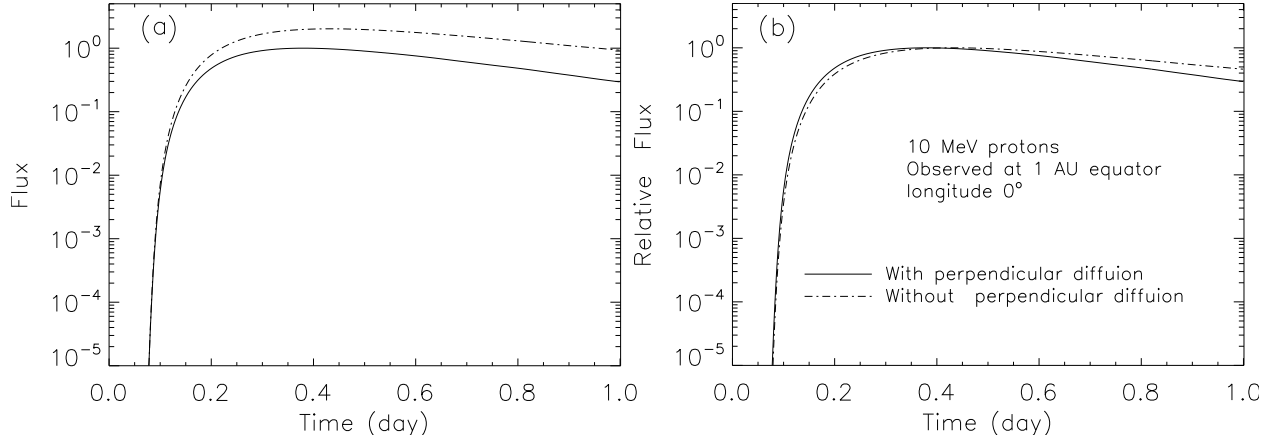


Fig. 1.— Comparison of 10 MeV proton fluxes with perpendicular diffusion (solid line) and without perpendicular diffusion (dash-dotted line).

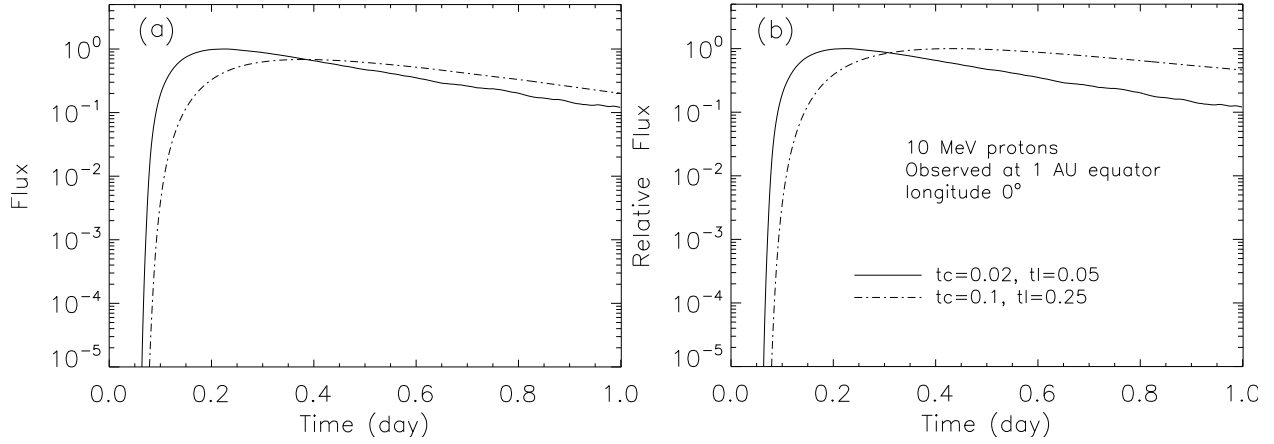


Fig. 2.— Comparison of 10 MeV proton fluxes with short source duration (solid line) and long source duration (dash-dotted line).

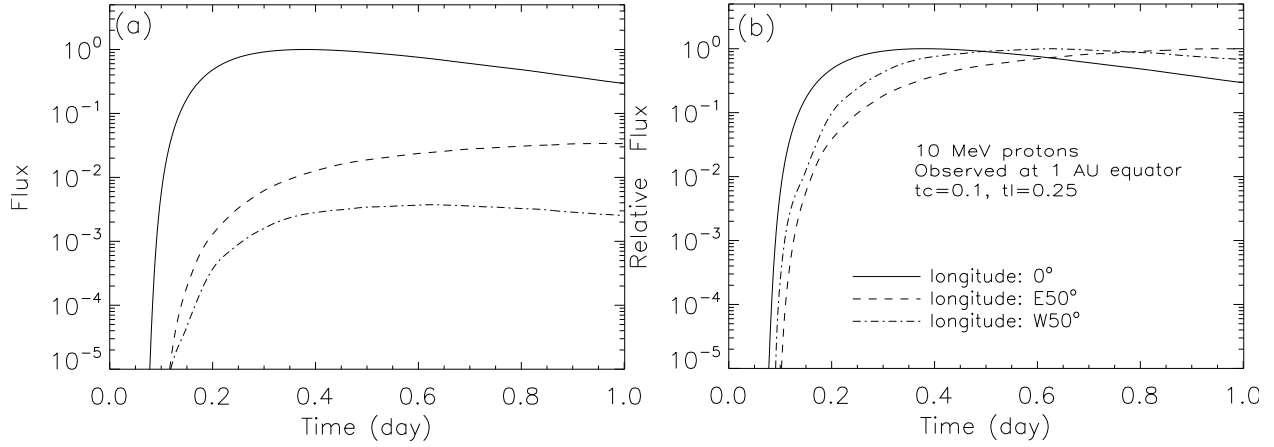


Fig. 3.— Comparison of 10 MeV proton fluxes observed at different locations. The $E50^\circ$ is short for 50° east, and $W50^\circ$ is short for 50° west.

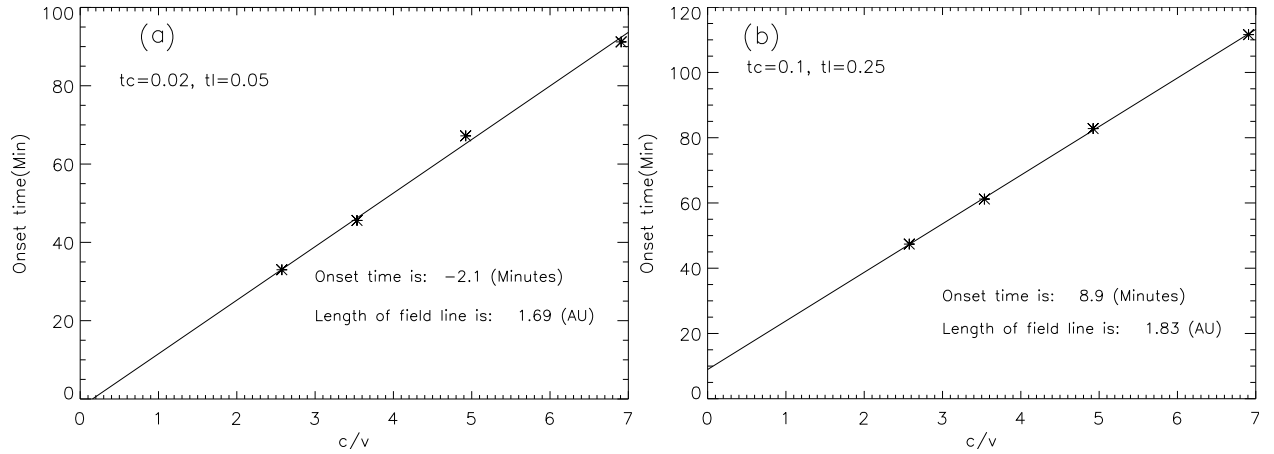


Fig. 4.— The results of using the VDA method to calculate the SEP release time and path length.

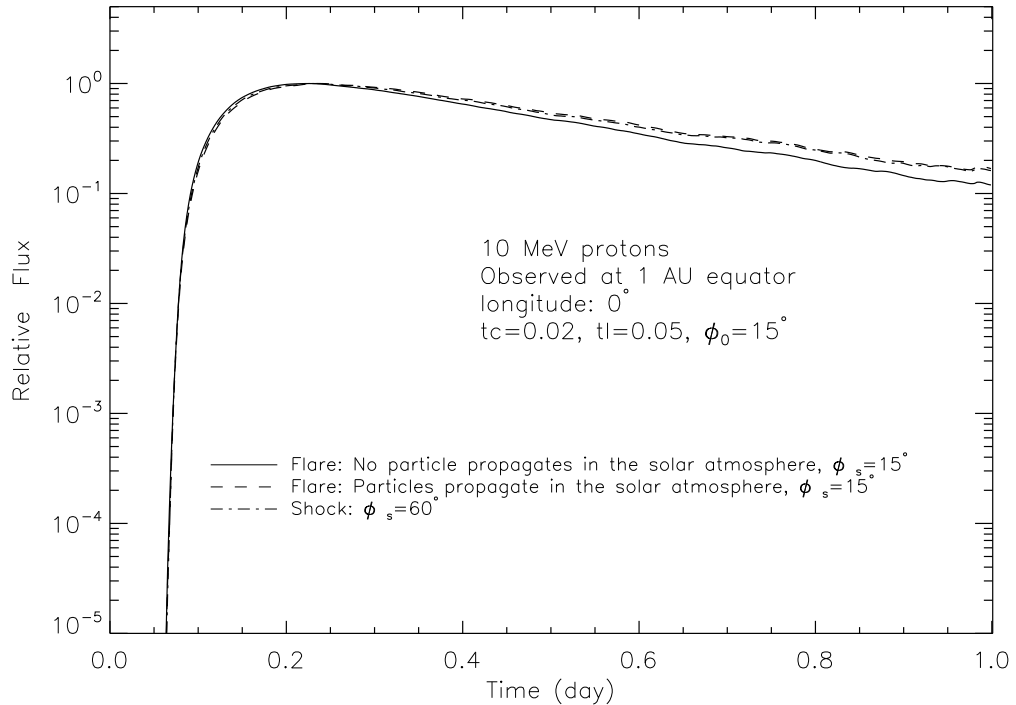


Fig. 5.— Comparison of 10 MeV proton fluxes observed at 1 AU which are produced by different SEP sources. The solid line indicates the case when particles are accelerated by flare, and particles do not propagate in the solar atmosphere. The dash line indicates the case when particles are accelerated by a flare, and particles can propagate in the solar atmosphere. The dash-dotted line indicates the case when particles are accelerated by a coronal shock.

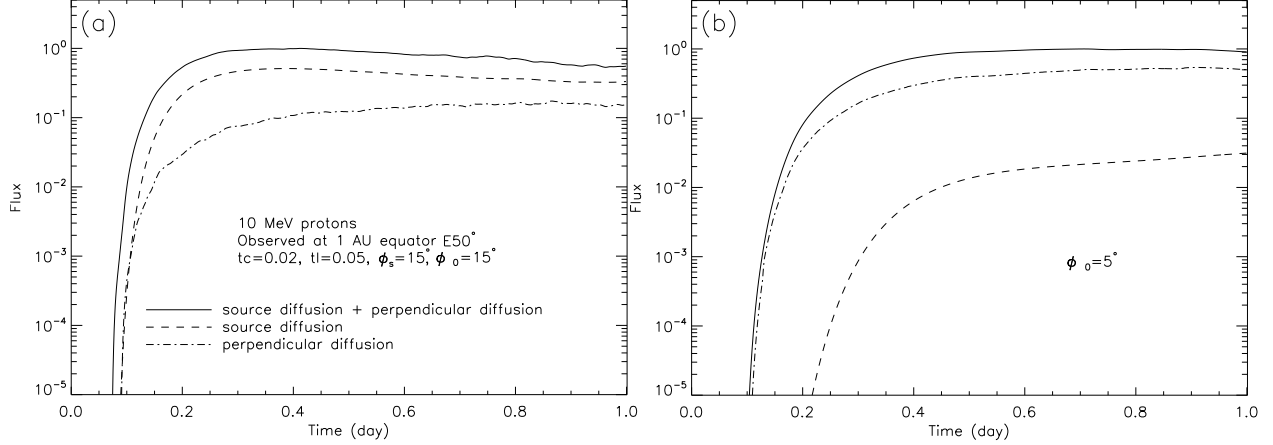


Fig. 6.— Comparison of 10 MeV proton fluxes in the cases with different propagation models. The solid lines indicate the case when particles can propagate in the solar atmosphere, and can also cross the field lines in the interplanetary space with perpendicular diffusion. The dashed lines indicate the case when particles can propagate in the solar atmosphere, but without perpendicular diffusion in the interplanetary space. The dash-dotted lines indicate the case when particles can cross the field lines in the interplanetary space with perpendicular diffusion, but without propagation in the solar atmosphere.

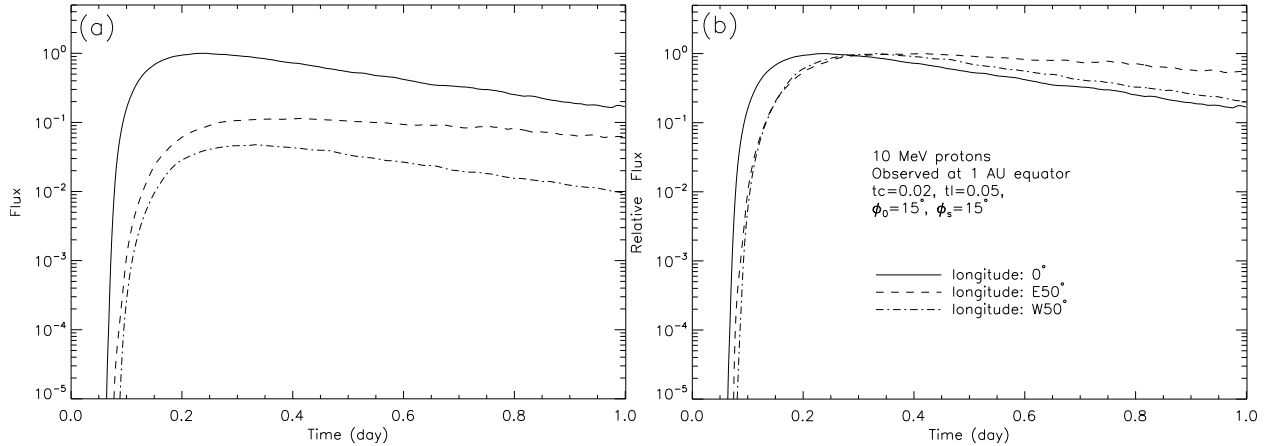


Fig. 7.— Comparison of 10 MeV proton fluxes observed at different locations. The particles are accelerated by a flare, and the ϕ_s is set to be 15° .

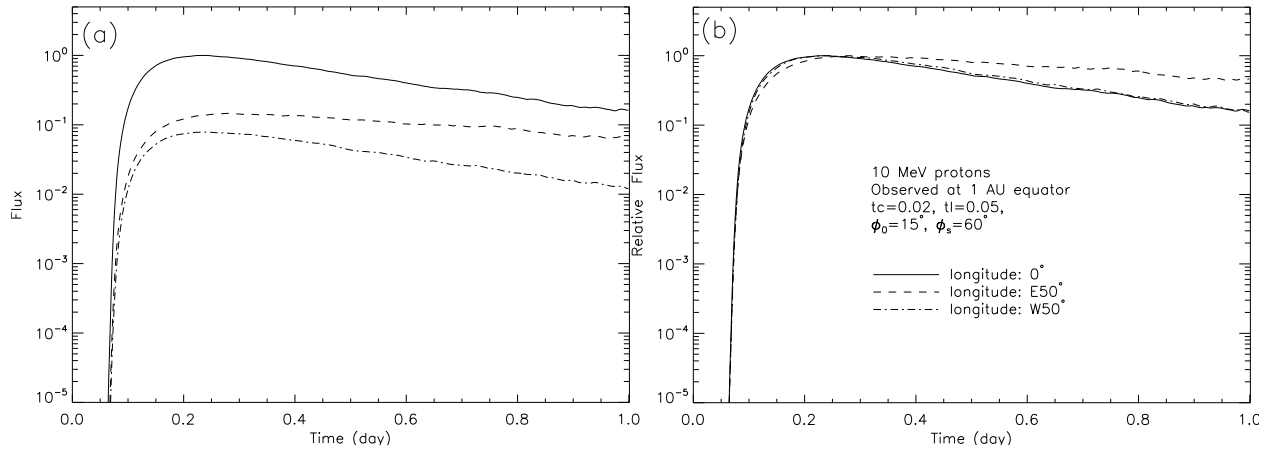


Fig. 8.— Comparison of 10 MeV proton fluxes observed at different locations. The particles are accelerated by a coronal shock, and the ϕ_s is set to be 60° .

Table 1: Results of VDA method.

Case	Duration	Background	Location	t_i (min)	L (AU)
1	Short	Low	Center	-2.1	1.69
			W50	-12	2.42
			E50	-18	2.51
2	Short	Middle	Center	-1.7	1.86
			W50	-8.3	2.38
			E50	-18	2.68
3	Short	High	Center	-0.98	2.34
			W50	-23	3.95
			E50	-43	4.83
4	Long	Low	Center	8.9	1.84
			W50	1.5	2.39
			E50	-8.9	2.70
5	Long	Middle	Center	12	2.09
			W50	9.9	2.66
			E50	-7.7	3.34
6	Long	High	Center	26	2.98
			W50	26	4.65
			E50	-6.9	6.45